SIMULATION OF FIRE SMOKE DISASTER IN A GOAF DURING THE CLOSURE PROCESS

by

Qiuling ZUO [a*] ***and Jingshan LI*** [b]

[a] College of Safety Engineering, Henan Institute of Engineering, Zhengzhou, China
[b] Public Security Department, Railway Police College, Zhengzhou, China

Original scientific paper
https://doi.org/10.2298/TSCI200630323Z

Closing the fire area is a common disaster-relief measure when coal spontaneously combusts in a goaf. However, the closure process will also increase the risk of gas explosion. To understand the gas migration rules and disaster-causing effects in a closed goaf, this study simulates the spontaneous combustion of leftover coal when the goaf is closed. The simulation was visualized on the PyroSim interface. After identifying the distribution laws of the temperature field, CO concentration field, and O_2 *concentration field, a disaster risk analysis was carried out the CO concentration presented two different changing trends over time. Both trends were approximately linear. A potential high temperature fire source was identified at depths of 50-60 m in the goaf (approximately 3 m above the floor). Before the goaf closure was completed, likely gas-explosion sites were found at depths of 30, 50, and 80 m from the working face. Monitoring the gas and oxygen concentrations is especially important in these areas.*

Key words*: closed goaf, smoke, disaster wind speed, CO concentration*

Introduction

Spontaneous combustion is one of five major goaf disasters in coal mines, and has always been a focus of mine safety research [1-3]. Sealing the goaf after spontaneous coal combustion is a common disaster-relief measure, but it also incurs a risk of gas explosion accidents. Moreover, as the actual environment of a goaf is somewhat complicated, accurately determining the distributions of the temperature field, CO concentration field, and O_2 concentration field in the goaf after spontaneous coal combustion is a difficult task. Quantifying the risk of gas explosion is also difficult. Current field and laboratory tests still cannot precisely reproduce the complex multi-field environment in a confined goaf. To assess the hazard risk during a coal fire, multiple mine-safety researchers have simulated the distributions of temperature, CO concentration, and O_2 concentration fields in the confined goaf. Such simulations provide a basis for the prediction and control of gas explosions in a confined goaf.

For many years, scholars have solved the flow field, elemental concentration fields, and temperature field in a goaf using universally available software (FLUENT, MATLAB, COMSOL) or independently developed software. Using the PyroSim fire-simulation soft-

[*] Corresponding author, e-mail: zuoqiuling@haue.edu.cn

ware, Wang *et al.* [4] simulated the changes of CO concentration, temperature and visibility while varying the flue gas parameters in the coal mining face. They investigated the effect of fire-source scale and wind speed. In another PyroSim study, Tian *et al.* [5] discussed the relationship between wind speed and fire spread in a mine. They derived a functional expression between the distance of the fire source and the wind speed at a stable temperature under exogenous fires of coal mines. In a CFD model, Yuan *et al*. [6] simulated the 3-D temperature increase during spontaneous coal combustion in a fixed goaf area. They reported the evolution process of spontaneous combustion in the goaf under dynamic advancement. Taraba *et al.* [7] also studied the spontaneous combustion of coal in a goaf under continuous advancement, and Lui *et al.* [8] studied the possibility of spontaneous combustion of large-flow CH_4 emissions in the goaf, combining dynamic permeability with Forchheimer's non-linear equation. They analyzed the 3-D oxygen distribution and heating law in the goaf. Zhang *et al.* [9] carried out a discrete element simulation on broken coal samples based on the bonded particle model (BPM), and reported the evolution characteristics of the stress, strain and fracture of broken coal in these goafs during compaction. To describe the crushing in the BPM during the compaction, they formulated a model to calculate the particle crushing rate. The crushing rate of soft coal was significantly higher than that of hard coal. Sipila *et al.* [10] discussed the risk, prevention and extinguishment of fires in enclosed coal storage facilities, drawing on experiences in the Finnish Salmisaari underground rock storage facility. They described the factors affecting fire risk, and outlined the related fault and event trees. Adam *et al.* [11] introduced a model developed by the French National Institute of Environmental and Industrial Hazards and the French National Central Institute for Environmental Studies. This model estimates the emissions from loosely mined and mined coal seams to longwall gobs. From the amount of emitted CH_4, the risk of CH_4 emissions from closed/sealed underground coal mines can be assessed. Zhou *et al.* [12] experimentally analyzed the factors influencing the gas explosion limit, proposed a new mixed combustible-gas explosion triangle, and created a new division of the inerting area. Their proposals provide a new analysis of gas explosions after sealing the fire zone. Niu *et al.* [13] proposed a dynamic control equation of the gas concentration in the fire zone, calculated different closing sequences of the coal-mine fire zone, and analyzed the combustion state before the fire zone is closed. Arif *et al.* [14] introduced tracer gas into underground mines, and analyzed its dispersion characteristics in a numerical simulation. From the concentration-time curve obtained from the measurements, they calculated the effective diffusion coefficient, which reflects the overall dispersion characteristics through the mine. Scott *et al.* [15] described the advantages and disadvantages of the two commonest underground longwall coal mining methods in Australia: chamber mining and pillar mining. They discussed the main geotechnical and operational issues and the factors to be considered when selecting a mining method, such as the changes in geological and geotechnical conditions induced by the method.

In all of the aforementioned researches, the fire in the closed area was caused by a fire outside the mine. Spontaneous combustion of coal in a closed goaf at different wind speeds has been rarely investigated. To provide this knowledge, the present study determines the temporal and spatial effects of spontaneous coal combustion in a closed goaf. The spontaneous combustion of coal under the most unfavorable conditions in the goaf are explored in large eddy simulations. At different wind speeds, the distribution laws of the temperature field, CO concentration field, and O_2 concentration field in the closed goaf are determined at face 21201, and the explosion risk posed by gas migration is assessed. The results can guide the management of goaf fire and gas during the fire period.

Construction of the spontaneous combustion model of coal in a closed goaf

Numerical model of spontaneously combusting coal fire

Closing a goaf to mitigate a fire disaster incurs a gas-explosion risk. The proposed simulation method of spontaneous coal combustion is based on the established physical model of the closed goaf [11]. The equations are:

$$-\nabla p = \frac{\mu}{k}v + \beta\rho\left|v\right|v \tag{1}$$

$$\nabla\left(-\frac{kH}{\mu+\rho\beta\left|v\right|}\nabla p\right) = Q_s \tag{2}$$

$$n\frac{\partial c_i}{\partial t} + v_i\nabla c_i - \nabla\left(nD_i\nabla c_i\right) = \frac{c-c_i}{c}W_i \tag{3}$$

$$\rho_\mathrm{e}c_\mathrm{e}\frac{\partial T}{\partial t} - \lambda_\mathrm{e}\nabla\left(\nabla T\right) + n\rho_g c_g v\nabla T = Q \tag{4}$$

where

$$\frac{1}{\lambda_\mathrm{e}} = \frac{1}{\lambda_g} + (1-n)\frac{1}{\lambda_m} \tag{5}$$

$$c_\mathrm{e} = nc_g + (1-n)c_m \tag{6}$$

$$\rho_\mathrm{e} = n\rho_g + (1-n)\rho_m \tag{7}$$

Calculation of coal spontaneous combustion parameters in the goaf

The spontaneous combustion of coal under the most unfavorable conditions in the goaf was simulated in PyroSim software. The main difficulty is determining the chemical reaction and related characteristic parameters of the coal. The goaf location was assumed as the typical location at which fires are more probable, spread at a faster rate, and exert a greater impact, than at other locations.

One-step reaction model of coal

In the developed model, the volatiles from coal particles during pyrolysis at intermediate temperatures are assumed to obey Arrhenius' law. A kinetic equation is then proposed. Schmidt [16] determined the molecular formula of coal as $C_{48}H_{65}SO_{26}$, with a molecular weight of 1089. The one-step chemical reaction of coal:

$$\mathrm{C_{48}H_{56}SO_{26} + 26O_2 = C_{26}H_{17}O_{10} + 24H_2O + SO_2 + 2CO + 20CO_2} \tag{8}$$

Coal pyrolysis rate under steady-state conditions

Coal undergoes spontaneous combustion. The combustion rate of coal in the pyrolysis process per unit area under steady-state conditions:

$$\dot{m}_f = \frac{\left(q_\mathrm{e} - q_L\right)A_\mathrm{v}}{L_V} = (15-11)\times\frac{1}{1.82} = 2.198 \tag{9}$$

Production rate of coal combustion products under steady-state conditions

The actual production rate of combustion product *j*:

$$\dot{G}_j = \eta_j \dot{m}_f k_j \tag{10}$$

In the one-step chemical reaction equation of coal, the production rates of CO_2 and CO are given, respectively:

$$k_{CO_2} = \frac{20 \times 48}{1089} = 0.808 \tag{11}$$

$$k_{CO} = \frac{2 \times 28}{1089} = 0.0514 \tag{12}$$

Inserting k_{CO} and k_{CO_2} into eq. (10), the actual production rates are obtained, respectively:

$$G_{CO_2} = 0.9 \times 2.198 \times 0.808 = 1.598 \tag{13}$$

$$G_{CO} = 0.0042 \times 2.198 \times 0.0514 = 0.000475 \tag{14}$$

Heat release rate of coal under steady-state conditions

The heat release rate is calculated:

$$Q_A = \frac{H_T}{k_{CO_2}} G_{co_2} + \left(\frac{H_T - H_{CO} k_{CO}}{k_{CO}} \right) G_{CO} = \frac{290}{0.808} 1.598 + \left(\frac{290 - 10 \times 0.0514}{0.0514} \right) 0.00047 = 573.8 \tag{15}$$

Physical model of the goaf

For the calculation, we selected the 21201 coal face of a coal mine, which is a *U*-shaped ventilation system. The ventilation rate was 1200 m^3 per minute, and the coal-seam gas content was 18 m^3 per minute. The wind resistance was 0.013 Ns^2/m^8. The mining was performed using a fully mechanized caving method. The height of the machine mining was 3.9 m, and the shortest spontaneous combustion period of the coal seam was 17.4 days. The mined area was 90 m long. The mixed gas temperature was 27 °C, and the average air density in the mine was 1.225 kg/m^3. The working-face width was 100 m. The air inlet and return roadways were 3 m wide. The thermal conductivity was 1.72 W/(m°C) in the coal and rock of the goaf, and 0.0264 W/(m°C) in the mixed gas in the goaf. The specific heat capacity was $5.12 \cdot 10^5$ J/(m^3°C) for the coal in the goaf, and 1206 J/(m^3°C) for the mixed air in the goaf. The initial temperature was 27 °C. The scale of the fire source was x = (20, 22), y = (60, 62), z = (0.5, 2.5), as shown in fig. 1.

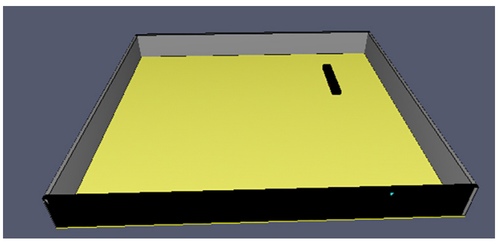

Figure 1. Physical model of the confined goaf

Results and discussion

The spontaneous combustion process of coal remaining in a closed goaf was analyzed in a PyroSim calculation using relevant coal parameters. The wind speed in the goaf continuously reduces during the closure process. In the simulation, the wind speed was set to 1.00

or 0.25 m/s, and the distributions of the CO concentration field, O_2 concentration field, and temperature field in the goaf were analyzed at each wind speed. The results of four analyses are presented and discussed below.

Distribution of CO concentration in the goaf at different wind speeds

The concentration distribution law in the goaf was explored at different depths (20, 30, 40, 50, 60, 70, and 80 m). At a goaf depth of 60 m, the concentration distributions were obtained at different heights (3, 5, 7, 9, and 10 m above the floor).

As shown in fig. 2, the CO concentration presented two different changing trends over time. Both change trends were approximately linear, but the increasing slope was much larger than the descending slope. At wind velocities of 1.00 and 0.25 m/s, the CO concentration was maximized at 20 and 80 m, respectively. At both wind velocities, the CO concentration was minimized at 50 m. This result indicates the likely presence of a high temperature fire source at 50 m deep in the goaf, which was burning in open-flame status.

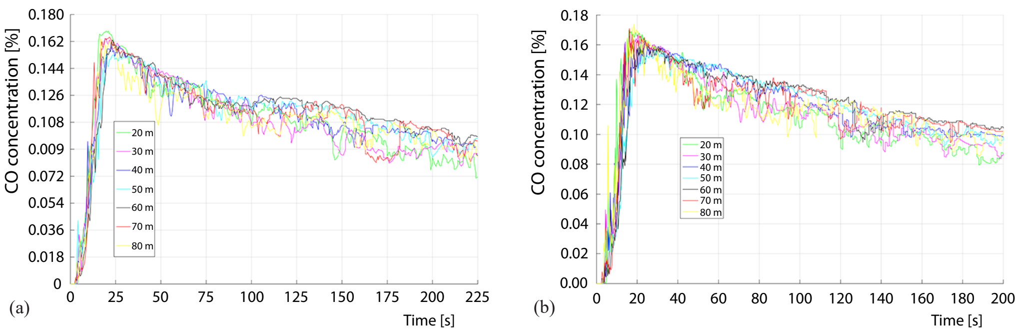

Figure 2. The CO concentration distributions at different depths in the goaf; (a) v = 1.00 m/s and (b) v = 0.25 m/s

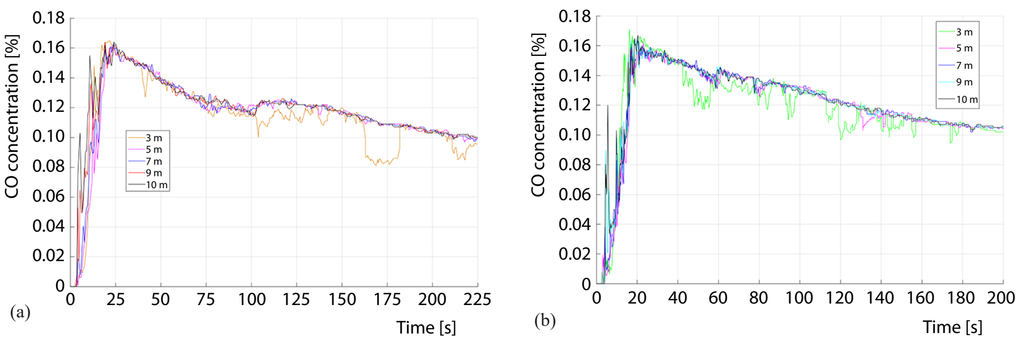

Figure 3. The CO concentration distributions at different heights in the goaf (depth = 60 m); (a) v = 1.00 m/s and (b) v = 0.25 m/s

Figure 3 plots the CO concentration trends at different heights at a goaf depth of 60 m. Again, the CO concentration initially rose and then declined. The slope was extremely sharp (approximately 80) in the rising region, and very gentle (0.33) in the falling region. At wind velocities of 0.25 and 1.00 m/s, the CO concentration was minimized at 9 and 10 m, respectively. At both wind velocities, the CO concentration was maximized at 3.0 m, indicating that the area around 3.0 m was a possible fire-source range at 60 m deep in the goaf. Combining the CO concentration distributions in figs. 2 and 3, the probable fire source was 50-60 m deep and 3.0 m above the bottom plate.

Distribution of O_2 concentration in the goaf at different wind speeds

This subsection discusses the oxygen concentration distributions at different depths (20-80 m at 10 m intervals) in the goaf, and at different heights (3-9 m at 2 m intervals and 10 m) at a goaf depth of 60 m.

The heat balance equation [16] was applied at the center of the experimental cavity.

As shown in fig. 4, the oxygen concentration in the goaf initially dropped rapidly from 20.9-3% at both wind speeds (1.00 and 0.25 m/s), and remained unchanged at later times. At a wind speed of 1.00 m/s, the oxygen concentration fluctuated at a depth of 50 m in the mined-out area, but at the lower wind speed (0.25 m/s), it fluctuated at multiple depths (30, 50, and 80 m) in the mined area. When coal seams with high gas content undergo spontaneous combustion, the gas concentration may reach 4-16% in the goaf. In predictions of the explosion hazard period in the goaf, the lower limit of explosive oxygen concentration is usually considered as 9%. In the present study, gas explosions before closure of the mined area were likely at depths of 30, 50, and 80 m. Therefore, the gas and oxygen concentrations must be monitored in these areas.

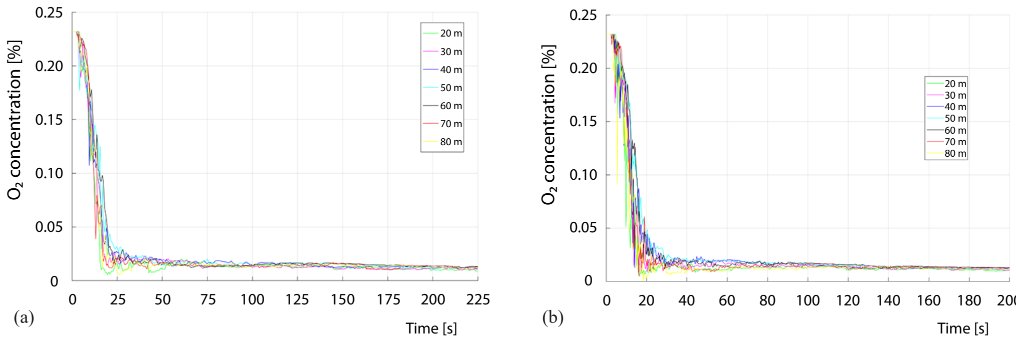

Figure 4. The O_2 concentration distributions at different depths in the goaf; (b) v = 1.0 m/s and (b) v = 0.25 m/s

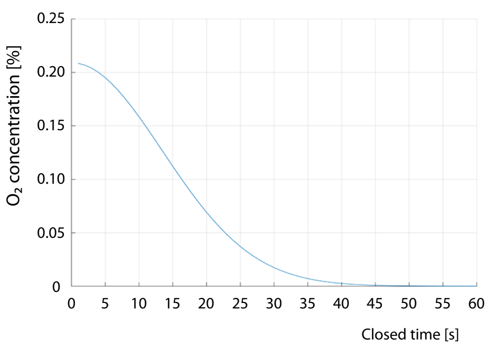

Figure 5. The O_2 concentration in the closed goaf during the first hour of fire-zone closure

By the principle of chemical reaction kinetics, the oxygen concentration after closing the goaf fire zone was modeled as an exponentially decaying function of time:

$$C_{O_2} = C_0 \times e^{-0.032bt^2} \tag{16}$$

The oxygen concentration in the fire zone during the first hour of closure is plotted in fig. 5.

As shown in fig. 5, the theoretical O_2 concentration decayed to zero after approximately 45 minutes of blocking time. Similar behavior was observed in the O_2 simulation study, fig. 4, confirming the reasonableness of the formula. After a blocking time of approximately 30 minutes, the O_2 concentration dropped to around 0.9%. When coal seams with high gas content undergo spontaneous combustion, the monitoring of harmful-gas concentrations in the goaf must be intensified within the first 30 minutes of closure to prevent gas explosions.

Temperature distribution in the goaf at different wind speeds

Next, the temperature distributions in the goaf were analyzed at different goaf depths (20-80 m at 10 m intervals), and at different heights (3-9 m at 2 m intervals and 10 m) at a goaf depth of 60 m.

As seen in fig. 6, the temperature distributions at wind speeds of 1.00 and 0.25 m/s initially increased and then decreased. The rise stage was rapid and approximately linear, whereas the decrease was more gradual and approximately logarithmic. At the high wind speed, the maximum temperature in the goaf decreased in the following order of mining depths (in m): 20 > 80 > 30 > 50 > 70 > 60 > 40. The maximum temperature ranged from 850 °C at 40 m to 1250 °C at 20 m. At the lower wind speed, the maximum temperature in the goaf decreased in the order 80 > 20 > 30 > 40 > 70 > 50 > 60 (all depths in m). The maximum temperature ranged from 810 °C at 60 m to 1200 °C at 80 m. When coal seams with high gas content undergo spontaneous combustion, explosion hazards are most likely at 20, 80, and 30 m from the working face. Combined with the distribution of O_2 concentration, this result suggests a greater possibility of gas explosion in these areas before closing the mined-out area. Therefore, the gas and oxygen concentrations must be intensively monitored at depths of 30 and 80 m.

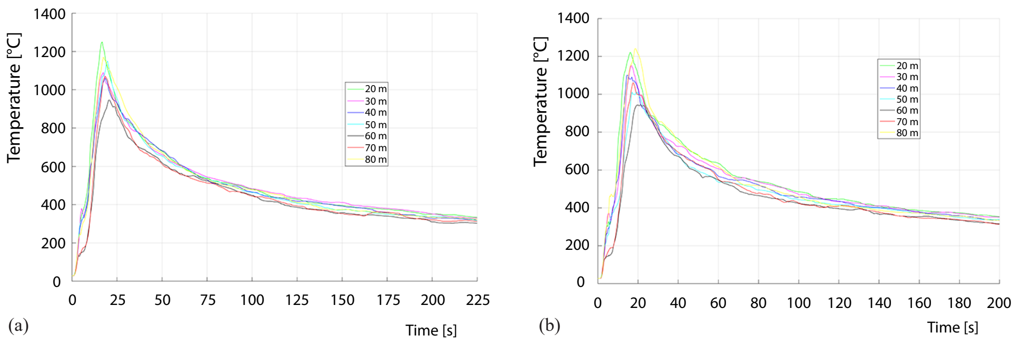

Figure 6. Temperature distributions at different depths in the goaf; (a) v = 1.00 m/s (b) v = 0.25 m/s

Analysis of smoke hazard in the goaf

After the spontaneous combustion of rich-gas coal seams and goaf closure, the CH_4 concentration in the confined goaf increased over time. The rate of gas accumulation gradually declined. Meanwhile, the oxygen concentration decreased over time, and finally settled at some low level. If the concentrations of both gases are within their respective explosion limits, a gas explosion occurs. Figure 7 plots the temporal changes in the internal gas concentrations after closure of the goaf.

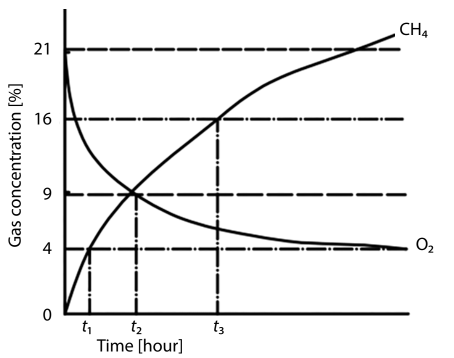

Figure 7. Relationship between the concentrations of O_2 and CH_4

In fig. 7, t_1 and t_3 denotes the time of reaching the upper and lower explosion limits of CH_4. When $t_1 < t < t_3$, the CH_4 concentration was within the explosive limit. Time t_2 in fig. 7 is the time at which the O_2 concentration reached its lower limit after closing the fire zone. The oxygen concentration met the explosive condition at $t < t_2$. Therefore, the likely period of a gas explosion is $(t_1 < t < t_3) \cap (t < t_2)$. If this intersection is empty, then no gas explosion occurs. If $t_2 < t_3$, the possible explosion time is $t_1 < t < t_2$; conversely, if $t_2 > t_3$, the possible explosion time is $t_1 < t < t_3$.

Conclusions

The conclusions of the study are summarized as follows.

- At different mining depths in the goaf, the CO concentration first increased and then decreased after closing off the fire zone. Both trends were approximately linear, but the increase was much faster than the decline. A possible high temperature fire source was identified at 50 m depth in the goaf, and approximately 3 m above the bottom plate.
- At wind speeds of 1.00 and 0.25 m/s, the oxygen concentration in the goaf dropped rapidly from 20.9% to 3.0%, and was unchanged thereafter. Before closing the goaf, a high possibility of gas explosion was identified at depths of 30, 50, and 80 m. The gas and oxygen concentrations should be carefully monitored in these areas.
- At wind speeds of 1.00 and 0.25 m/s, the temperature exhibited a rapid and approximately linear rise stage, followed by a more gradual and approximately logarithmic decline. When coal seams with high gas content spontaneously combust, the vulnerable sites of explosion hazard were identified at 20, 80, and 30 m from the working face. Before closing the mined-out area, the distribution of O_2 concentration implied that monitoring the gas and oxygen concentrations is especially important at depths of 30 and 80 m.
- When rich-gas coal seams spontaneously combust and abnormal CO concentrations are detected in the mined-out area, the gas must be drained from the working face until the explosion hazard in the enclosed area is mitigated. In addition, nitrogen can be drilled and injected from the safe area to the fire area. This measure would reduce the oxygen concentration in the enclosed area, preventing gas explosion and ensuring the safe closure of the fire area.

Acknowledgment

This work was funded by the National Natural Science Foundation of China (Grant No. 51904089). The authors wish to thank this organization for the support provided. They also wish to thank the reviewers and editors for their constructive comments and suggestions in improving the manuscript.

Nomenclature

A_v – surface area of combustible material, (= 1.0 m^2)
b – identification level, [–], (= 0.0864)
C_O – oxygen concentration before the goaf is closed, (= 20.9%)
C_{O_2} – oxygen concentration, [%]
c – concentration of gas in the goaf, [molm^{-3}]
c_e – equivalent volume specific heat capacity of coal and rock in goaf, [Jm^{-3}°C^{-1}]
c_i – concentration of mixed gas i in the goaf, [molm^{-3}]
c_m – volume specific heat capacity of coal and rock in goaf, [Jm^{-3}°C^{-1}]
c_g – specific heat capacity of air, [Jm^{-3}°C^{-1})
D_i – diffusion coefficient of mixed gas i in the goaf, [m^{2}s^{-1}]
G_j – actual production rate, [gm^{-2}s^{-1}]
H – coal-rock fall height, [m]
H_T – amount of heat released by complete combustion of coal per unit mass (= 290 KJg^{-1})
k – permeability coefficient, [m^{2}Pa^{-1}s^{-1}]
k_j – theoretical maximum production of component j of combustion products per unit mass, [–]
L_v – latent heat of coal volatilization (= 1.82 kJ kg^{-1})

m_f – combustion rate, [$gm^{-2}s^{-1}$]
n – void ratio, [–]
p – mixed-gas pressure in goaf, [Pa]
Q – goaf heat source [–]
Q_A – heat release rate, [kW]
Q_s – source (sink) of the leaking gas in the goaf, [–]
q_e – external heating flow rate per unit surface area of combustible material, (= 15 kWm^{-2})
q_L – gradiant heat loss per unit surface area of combustible material, (= 11 kWm^{-2})
T – temperature, [°C]
t – closing time, [s]
v – velocity, [ms^{-1}]
v – gas velocity in coal body, [ms^{-1}]
$|v|$ – modeled gas velocity in coal [–]
W_i – gas source i reacting in the goaf [–]

Greek symbols

β – non-Darcy flow factor, [m^{-1}]
η_j – production efficiency of products in the combustion process, ($\eta CO = 0.0042$, $\eta CO_2 = 0.9$)
λ_e – equivalent thermal conductivity of coal and rock in goaf, [$Wm^{-1}°C^{-1}$]
λ_m – thermal conductivity of coal and rock in goaf, [$Wm^{-1}°C^{-1}$]
λ_g – thermal conductivity of mixed gas, [Wm–1°C^{-1}]
μ – dynamic viscosity of flowing gas, [Pas]
ρ – flowing gas density, [kgm^{-3}]
ρ_e – equivalent density of mixed gas in goaf, [gcm^{-3}]
ρ_m – coal and rock density in goaf, [gcm^{-3}]
ρ_g – air density, [gcm^{-3}]

References

[1] Choi, H. Y., *et al*., Comparison of Spontaneous Combustion Susceptibility of Coal Dried by Different Processes from Low-Rank Coal, *Korean Journal of Chemical Engineering*, *31* (2014), 12, pp. 2151-2156
[2] Deng, J., *et al*., Effects of Pyrite on the Spontaneous Combustion of Coal, *International Journal of Coal Science & Technology*, *2* (2015), 4, pp. 306-311
[3] LU, W., *et al*.,. Method for Prevention and Control of Spontaneous Combustion of Coal Seam and Its Application in Mining Field, *International Journal of Mining Science and Technology*, *27* (2017), 5, pp. 839-846
[4] Wang, J. G., *et al*., Numerical Simulation of Smoke Variation During Fire in Intake Airways on a Coal Mining Face, *Proceedings*, 11th International Mine Ventilation Congress, (ed. Chang, X.), Xi'an, China, 2019, Vol. 1, pp. 652-663
[5] Tian, S. C., *et al*., Pyrosim-Based Wind Speed on the Spread of Mine Fires (in Chinese), *Metal Mine*, *2* (2020), pp. 199-205
[6] Yuan, L., *et al*., Computational Fluid Dynamics Study on the Ventilation Flow Paths in Long Wall Gobs, *Proceedings and Monographs in Engineering: Water and Earth Sciences*, *1* (2006), June, pp. 547-558
[7] Taraba, B., *et al*., Effect of Long Wall Face Advance Rate on Spontaneous Heating Process in the Gob Area-CFD Modelling, *Fuel*, *90* (2011), 8, pp. 2790-2797
[8] Liu, X. K., *et al.*, Simulation of Goaf Heating Law and the Fire Cooling Effect during Methane Drainage in High Level Laneway, *Journal of Coal Science and Engineering*, *19* (2013), 3, pp. 325-331
[9] Zhang, C., *et al*., Numerical Simulation of Broken Coal Strength Influence on Compaction Characteristics in Goaf, *Natural Resources Research*, *29* (2020), Jan., pp. 2495-2511
[10] Sipila, J., *et al*., Risk and Mitigation of Self-Heating and Spontaneous Combustion in Underground Coal Storage, *Journal of Loss Prevention in the Process*, *25* (2012), 3, pp. 617-622
[11] Adam, D., *et al*., Forecast of Methane Emission from Closed Underground Coal Mines Exploited by Long-wall Mining: A Case Study of Anna Coal Mine, Journal of Sustanable Forestry, *17* (2018), 4, pp. 184-194
[12] Zhou, X., *et al*., Influences of Sealing Fire Zone in High Gas Mine on Impact Factors of Gas Explosion Limit, *Combustion, Explosion, and Shock Waves*, *33* (2013), 4, pp. 351-356
[13] Niu, H., *et al*., Influence of Closed Sequence on Distribution of Gas in Coal Mine Fire Zone, *Journal of Central South University*, *47* (2016), 9, pp. 3239-3245
[14] Arif, W., *et al*., Assessment of Air Dispersion Characteristic in Underground Mine Ventilation: Field Measurement and Numerical Evaluation, *Process Safety and Environmental Protection*, *93* (2015), 1, pp. 173-181
[15] Scott, B., *et al*., Geological and Geotechnical Aspects of Underground Coal Mining Methods within Australia, *Environmental Earth Sciences*, *60* (2010), Aug., pp. 1007-1019
[16] Schmidt, M., et al., Self-Innition of Dust at Redued Volume Frations of Ambient Oxygen, *Journal of Loss Prevention in the Process Industries*, *16* (2003), 2, pp. 141-147

Paper submitted: June 30, 2020
Paper revised: September 5, 2020
Paper accepted: September 25, 2020